Bilayer processing for an enhanced organic-electrode contact in ultrathin bottom contact organic transistors

Jeongwon Park, Richard D. Yang, Corneliu N. Colesniuc, Amos Sharoni, Sungho Jin, Ivan K. Schuller, William C. Trogler, and Andrew C. Kummel[a]

Integrated Nanosensor Lab, Materials Science and Engineering Program, Department of Physics and Department of Chemistry and Biochemistry, University of California, San Diego, La Jolla, California 92093, USA

A bilayer lift-off process has been employed to fabricate optimal electrode contact geometry for statistical characterization of ultrathin organic thin-film transistors (OTFTs). For over 100 *p*-channel ultrathin (12 ML) copper phthalocyanine (CuPc) OTFTs, the bilayer photoresist lift-off process increased the field effect mobility by two orders of magnitude, decreased the contact resistance by three orders of magnitude, increased the on/off ratio by one order of magnitude, and the threshold voltage was decreased by a factor of three compared to conventionally processed devices. The generality of the method was validated by fabricating OTFTs in four different phthalocynaines and CuPc OTFTs with eight different channel thicknesses. © *2008 American Institute of Physics*. [DOI: 10.1063/1.2918121]

Organic thin-film transistors (OTFTs) have received increasing attention because of their potential applications in displays, optoelectronics, logic circuits, and sensors.[1–5] Ultrathin OTFTs are of technical interest as a possible route toward reduced bias stress in standard OTFTs[6,7] and enhanced sensitivity in chemical field-effect transistors (chemFETs).[8] ChemFETs are OTFTs whose output characteristics are sensitive to the presence of analytes via changes in the channel mobility and/or threshold voltage induced by analyte chemisorption onto the channel materials. Previous studies of the charge injection process from the metal contact to the conduction channel in OTFTs show that carriers primarily conduct through a few monolayers above the gate dielectric.[9] Due to such a conduction mechanism, the contact between the electrode and the metal phthalocyanine (MPc) layer significantly affects the carrier transport behavior of organic films.[10]

This study reports a fabrication method for ultrathin OTFTs, which provides a low contact resistance between an MPc channel and the source/drain electrodes. The channel profile becomes critical for ultrathin devices in which the organic channel thickness is smaller than the height of the electrodes. Utrathin thin channels are favorable for chemFETs because they exhibit far lower drift, thereby making superior sensors.[6] We show that enhanced electrical properties can be achieved by employing a bilayer photoresist lift-off process,[11–15] which sculpts the contact morphology at the edge of the electrodes.

Bottom-contact OTFTs were prepared by either the standard, single layer lift-off processing [Fig. 1(a)] or a bilayer lift-off processing [Fig. 1(b)], on thermally grown SiO_2 (100 nm thickness) on (100) n^+ Si substrates. The channel length was defined by photolithography to be 5 μm. In the bilayer photoresist lift-off process, two different types of photoresist material with distinct etching rates are utilized: polymethylglutarimide (PMGI) as the bottom resist layer and Microposit® S1805 photoresist as the top resist layer. The underlying PMGI resist layer nearly isotropically develops

and etches faster in the Microposit® MF319 developer solution (Shiplay Corp.) than the top layer S1805. Therefore, the amount of undercut is precisely controlled by the etching rate of PMGI [see Fig. 1(b)]. The source and drain electrodes are deposited with the use of electron beam evaporation at a rate of 1 Å/s. A 5 nm thick Ti adhesion layer was applied first, followed by deposition of 45 nm thick Au for a total electrode thickness of 50 nm. For the bilayer resist process on the 12 ML CuPc chemFETs, 18 chips each containing six devices were fabricated. For the single resist process on the 12 ML CuPC chemFETs, 13 chips each containing six devices were fabricated.

Shown in Figs. 1(c) and 1(d) are the scanning electron microscopy (SEM) images of typical electrodes after the single layer photoresist lift-off process and after the bilayer photoresist lift-off process. A total of ten electrodes, each on a different device, were examined by SEM and all of them had nearly identical structures to those displayed in Figs. 1(c) and 1(d). The contact angles between the electrodes and the SiO_2 were measured for ten electrodes of each type. The contact angles are $+133.2 \pm 13.8°$ and $+51.2 \pm 7.8°$ for the single layer lift-off and bilayer lift-off process devices, respectively. The SEM data show that the single layer lift-off
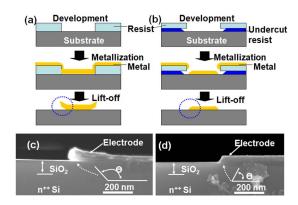

FIG. 1. (Color online) Outlines of the OTFT fabrication process using (a) single layer photoresist process and (b) bilayer photoresist process. SEM images of the electrodes (c) after single layer photoresist lift-off processing and (d) after bilayer photoresist lift-off processing.

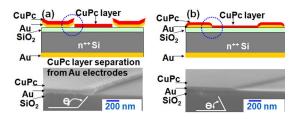[a]Electronic mail: akummel@ucsd.edu.

FIG. 2. (Color online) CuPc and electrode configurations in OTFTs. Top: schematic structures, Bottom: the SEM images after depositing 12 ML CuPc (a) Undesirable electrical separation of ultrathin organic layer from the electrode in single photoresist lift-off processing. (b) Enhanced electrical contacts with bilayer photoresist lift-off processing.

process produces an electrode with elevated edges while the double layer lift-off process produces a tapered electrode with the edges in contact with the substrate surface. The MPc deposition processes have been described elsewhere.[5,6] Briefly, controlled thickness layer of MPc[16,17] were deposited by organic molecular beam epitaxy (OMBE) with the substrate temperature kept at 25 °C (see EPAPS document).[17]

Shown in Fig. 2 are the cross-sectional views of OTFT structures and typical SEM images after depositing 12 ML of CuPc on the electrodes of Figs. 1(c) and 1(d). A total of ten electrodes, each on a different device, were examined by SEM and 100% had nearly identical structures to those displayed in Figs. 2(c) and 2(d). The contact angles between the electrodes and the SiO_2 after CuPc deposition are $+136 \pm 10.1°$ and $+40 \pm 4.4°$ for the single layer lift-off and bilayer lift-off process devices, respectively. As shown in Fig. 2(a), the single layer lift-off processed devices have electrodes that are physically detached from the organic channel. Conversely, the bilayer lift-off processed devices shown in Fig. 2(b) have a smooth contact between the source/drain metal electrodes and organic channel.

The OTFT devices were characterized in an optically isolated probe station at 25 °C to minimize photocurrent. Figures 3(a) and 3(b) show the representative plots of source-drain current (I_{ds}) versus source-drain voltage (V_{ds}) at different gate-source voltages (V_{gs}) from +8 to −12 V. The output characteristics of the 12 ML CuPc OTFTs, using the
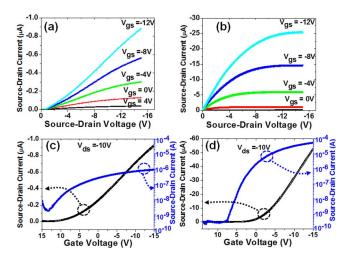

FIG. 3. (Color online) *I-V* characteristics of OTFTs (a) OTFTs by conventional single layer photoresist process. (b) OTFTs with bilayer photoresist lift-off process. (c) Transfer characteristics for OTFTs with single layer photoresist process, $V_{ds} = -10$ V. (d) Transfer characteristics for OTFTs obtained with the bilayer photoresist process, $V_{ds} = -10$ V. In the transfer curve, the source-drain current below 10^{-8} A is affected by the gate leakage current.

single layer photoresist lift-off process show a *p*-type behavior with a lack of current saturation. Conversely, with the bilayer photoresist lift-off process, the linear region and the saturation region are observed clearly. Figures 3(c) and 3(d) represent the typical transfer curves of 12 ML CuPc OTFTs at a fixed V_{ds} of −10 V for the single layer lift-off versus the bilayer lift-off devices. All the devices were *p*-channel transistors and all the bilayer lift-off devices had good Ohmic behavior at low voltages as demonstrated by the intercept at the origin and the saturated current at high V_{ds} shown in Fig. 3(b). Conversely, the transfer curves from the single layer lift-off devices are consistent with an OTFT with a poor on-off ratio and poor subthreshold performance.

The electrical parameters were measured on 79 12 ML CuPc OTFTs fabricated with the bilayer lift-off process and 41 12 ML CuPc OTFTs using the single layer lift-off process; the results are summarized in Table I. 91% of the bilayer lift-off processed devices had measurable electronic properties. The failures of 9% of the devices were mostly due to gate leakage. We only obtained measurable electrical properties from 41 OTFTs out of 78 (53%) for devices fabricated using the single layer lift-off process, primarily due to poor reliability of the contacts.

The field effect mobilities were extracted from the linear region $[V_{ds} \ll (V_{gs} - V_{th})]$ of the I_{ds} versus V_{ds} plots for each device (Ref. 18).

The field effect mobility values (mean $\pm$ standard deviation) extrapolated from the linear region are $(3.4 \pm 4.9) \times 10^{-6}$ and $(6.1 \pm 1.3) \times 10^{-4}$ cm^2/V s for the single layer lift-off processed and the bilayer lift-off processed devices, respectively. The large difference in extrapolated field effect mobility values is consistent with a non-negligible parasitic resistance associated with the channel-electrode contacts. Furthermore, there was one order of magnitude difference in on/off ratio between the single layer lift-off processed and the bilayer lift-off processed devices ($6.0 \times 10^3 - 4.5 \times 10^4$). This increase in mobility and on/off ratio is consistent with a lower contact resistance in the bilayer photoresist process devices. The contact resistance can be extracted by determining R_{on} from the linear region of the output characteristics.[19] The contact resistance values calculated from the linear region at fixed gate voltage ($V_{gs} = -12$ V) are $(1.84 \pm 2.14) \times 10^8$ Ω and $(9.61 \pm 3.90) \times 10^4$ Ω ohm for the single layer lift-off processed and the bilayer lift-off processed devices, respectively. The threshold voltages were extracted in the linear region by linearly extrapolating the transfer curves between $V_{gs} = -5$ to -15 V.[18] The threshold voltages are $+5.7 \pm 4.7$ and $+2.2 \pm 1.1$ V for the single layer lift-off and bilayer lift-off processed devices, respectively.

As shown in Table I, the analysis of the standard deviations of the electrical parameters show that the fractional standard deviation of the mobility and on-current are lower for the bilayer lift-off processed devices compared to the single lift-off processed devices, which is consistent with the former process being more uniform. The relatively narrow distributions of electrical properties in the bilayer lift-off process devices are consistent with better control of the electrode profile in the first few nanometers above the surface.

The variation of the field effect mobility of ultrathin OTFTs as a function of contact resistance are shown in Fig. 4. The field effect mobility consistently decreased with increasing contact resistance in the bilayer lift-off processed ultrathin OTFTs. Additionally, the intrinsic mobility obtained

TABLE I. Comparative electrical characteristics of organic thin film transistors based on single layer vs bilayer photoresist lift-off process. Mobilities extracted from the linear region, on/off ratio obtained from the drain current for $V_{gs}=15$ V to $V_{gs}=-15$ V. The on-state current was calculated from the drain current at fixed $V_{gs}=-15$ V and $V_d=-10$ V. The electrical parameters were measured on 79 OTFTs fabricated with the bilayer lift-off process and 41 OTFTs using the single layer lift-off process. SD is the standard deviation while SE is the standard error.

	Bilayer photoresist lift-off process					Single layer photoresist lift-off process				
	Mean	SD	SD (%)	SE	SE (%)	Mean	SD	SD (%)	SE	SE (%)
V_T (V)	2.23	1.09	49	0.12	5	5.71	4.7	82	0.73	12
μ (cm²/V s)	6.08×10^{-4}	1.27×10^{-4}	21	1.43×10^{-5}	2	3.45×10^{-6}	4.91×10^{-6}	142	7.67×10^{-7}	22
R_c (Ω)	9.61×10^{4}	3.90×10^{4}	41	4.39×10^{3}	5	1.84×10^{8}	2.14×10^{8}	116	3.38×10^{7}	18
I_{on} (A)	4.13×10^{-5}	7.37×10^{-6}	18	8.30×10^{-7}	2	4.46×10^{-7}	7.02×10^{-7}	157	1.1×10^{-7}	24
I_{on}/I_{off}	4.5×10^{4}	6.0×10^{4}	132	6.7×10^{3}	15	6.0×10^{3}	9.4×10^{3}	157	1.5×10^{3}	25

from the zero contact resistance intercept of the linear fit to data for bilayer lift-off process devices was 8.9×10^{-4} cm²/V s at room temperature, which is comparable to the best values of mobility of bottom contact CuPc OTFTs with longer channels (12–25 μm) and thicker CuPc layers (50–60 nm).[20] For single layer lift-off processed ultrathin OTFTs, there is an approximately exponential correlation between the field effect mobility and contact resistance. The strong correlation between contact resistance and mobility is consistent with the contact resistance being the primary cause of reduced electrical performance in these ultrathin OTFTs.

The generality of the method was validated by fabricating OTFTs in four different phthalocynaines (CuPc, NiPc, H$_2$Pc, and CoPc) and CuPc OTFTs with eight different channel thicknesses (4–1047 ML).[17] The contact resistance values (mean ± standard deviation) with different phthalocyanines are $(9.6\pm3.9)\times10^{4}$ Ω (CuPc, 12 ML), $(4.8\pm3.4)\times10^{4}$ Ω (NiPc, 12 ML), $(2.5\pm0.7)\times10^{5}$ Ω (H$_2$Pc 12 ML), and $(1.4\pm1.4)\times10^{5}$ Ω (CoPc, 12 ML). The contact resistance values with different CuPc thicknesses are $(3.9\pm3.9)\times10^{6}$ Ω (4 ML), $(9.6\pm3.9)\times10^{4}$ Ω (12 ML), $(1.60\pm0.4)\times10^{6}$ Ω (36 ML), $(1.20\pm0.6)\times10^{6}$ Ω (100 ML), $(5.4\pm2.6)\times10^{5}$ Ω (150 ML), $(6.4\pm1.4)\times10^{5}$ Ω (250 ML), $(6.9\pm0.9)\times10^{5}$ Ω (494 ML), and $(2.8\pm1.6)\times10^{5}$ Ω (1047 ML) for the bilayer lift-off processed CuPc devices. The higher contact resistance of the 4ML CuPc devices may be due to incomplete film coverage above the third layer or differences in film texture.[6] As compared with the contact resistance on the single layer lift-off processed electrodes $[(1.8\pm2.1)\times10^{8}$ Ω, CuPc, 12 ML], the bilayer photoresist lift-off process on different phthalocyanines and different CuPc thicknesses decreased the contact resistance by be-

tween two and three orders of magnitude. Furthermore, all of fabricated OTFTs using the bilayer lift-off process showed the clear saturation behavior.

In summary, ultrathin, OTFTs with significantly improved properties have been produced using a bilayer lift-off photoresist process. The results were consistent with a careful tapering of the electrodes, being a requirement for high performance in ultrathin OTFTs. The observed improvements in mobility, I_{on}/I_{off} ratio and threshold voltage indicate the crucial role of interface contacts in charge transport in bottom-contact OTFTs.
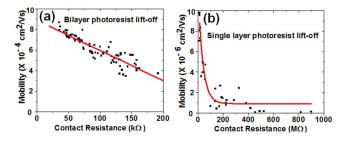
FIG. 4. (Color online) Field effect mobility vs contract resistant of the OTFTs (a) bilayer photoresist processed OTFTs and (b) single layer photoresist processed OTFTs.

[1] C. D. Dimitriakopoulous and P. R. L. Malenfant, Adv. Mater. (Weinheim, Ger.) **14**, 99 (2002).
[2] M. Bouvet, Anal. Bioanal. Chem. **384**, 366 (2006).
[3] K. A. Miller, R. D. Yang, M. J. Hale, J. Park, B. Fruhberger, C. N. Colesniuc, I. K. Schuller, A. C. Kummel, and W. C. Trogler, J. Phys. Chem. B **110**, 361 (2006).
[4] F. I. Bohrer, A. Sharoni, C. Colesniuc, J. Park, I. K. Schuller, A. C. Kummel, and W. C. Trogler, J. Am. Chem. Soc. **129**, 5640 (2007).
[5] R. D. Yang, B. Fruhberger, J. Park, and A. C. Kummel, Appl. Phys. Lett. **88**, 074104 (2006).
[6] R. D. Yang, T. Gredig, C. N. Colesniuc, J. Park, I. K. Schuller, W. C. Trogler, and A. C. Kummel, Appl. Phys. Lett. **90**, 263506 (2007).
[7] S. J. Zilker, C. Detcheverry, E. Cantatore, and D. M. de Leeuw, Appl. Phys. Lett. **79**, 1124 (2001).
[8] R. D. Yang, J. Park, C. N. Colesniuc, I. K. Schuller, W. C. Trogler, and A. C. Kummel, J. Appl. Phys. **102**, 034515 (2007).
[9] G. Horowitz, J. Mater. Res. **19**, 1946 (2004).
[10] R. Schmechel and H. von Seggern, Phys. Status Solidi A **201**, 1215 (2004).
[11] A. Talin, G. F. Cardinale, T. I. Wallow, P. Dentinger, S. Pathak, D. Chinn, and D. R. Folk, J. Vac. Sci. Technol. B **22**, 781 (2004).
[12] L. An, Y. Zheng, K. Li, P. Luo, and Y. Wu, J. Vac. Sci. Technol. B **23**, 1603 (2005).
[13] M. J. Rooks, C. C. Eugster, J. A. del Alamo, G. L. Snider, and E. L. Hu, J. Vac. Sci. Technol. B **9**, 2856 (1991).
[14] B. P. Van der Gaag and A. Scherer, Appl. Phys. Lett. **56**, 481 (1990).
[15] T. Ishii, H. Nozawa, and T. Tamamura, Appl. Phys. Lett. **70**, 1110 (1997).
[16] C. W. Miller, A. Sharoni, G. Liu, C. N. Colesniuc, B. Fruhberger, and I. K. Schuller, Phys. Rev. B **72** 104113 (2005).
[17] See EPAPS Document No. E-APPLAB-92-098817 for the OMBE deposition processes, molecular structure and surface morphology of CuPc. For more information on EPAPS, see http://www.aip.org/pubservs/epaps/.html.
[18] D. K. Schroder, *Semiconductor Material and Device Characterization* (Wiley, New York, 1998).
[19] S. Luan and G. W. Neudeck, J. Appl. Phys. **72**, 766 (1992).
[20] Z. Bao, A. J. Lovinger, and A. Dodabalapur, Appl. Phys. Lett. **69**, 3066 (1996).